CHALMERS
UNIVERSITY OF TECHNOLOGY

Impact of Mesh Density and Time-Step Variation on Losses and Torque Characteristics in 3D and 2D FEM Models of an Axial Flux Machine

Downloaded from: https://research.chalmers.se, 2026-05-02 02:11 UTC

Citation for the original published paper (version of record):
Puttaraj, V., Tidblad Lundmark, S., Thiringer, T. (2025). Impact of Mesh Density and Time-Step Variation on Losses and Torque Characteristics in 3D and
2D FEM Models of an Axial Flux Machine. 2025 IEEE 4th Industrial Electronics Society Annual On-Line Conference (ONCON). http://dx.doi.org/10.1109/ONCON68412.2025.11384185

N.B. When citing this work, cite the original published paper.

© 2025 IEEE. Personal use of this material is permitted. Permission from IEEE must be obtained for all other uses, in any current or future media, including reprinting/republishing this material for advertising or promotional purposes, or reuse of any copyrighted component of this work in other works.

(article starts on next page)

Impact of Mesh Density and Time-step Variation on Losses and Torque Characteristics in 3D and 2D FEM Models of an Axial Flux Machine

Vineetha Puttaraj
Department of Electrical Engineering
Chalmers University of Technology
Gothenburg, Sweden
vineetha@chalmers.se or

Sonja Tidblad Lundmark
Department of Electrical Engineering
Chalmers University of Technology
Gothenburg, Sweden
sonja.lundmark@chalmers.se or

Torbjörn Thiringer
Department of Electrical Engineering
Chalmers University of Technology
Gothenburg, Sweden
torbjorn.thiringer@chalmers.se or

2025 IEEE 4th Industrial Electronics Society Annual On-Line Conference (ONCON) | 979-8-3315-8964-6/25/$31.00 ©2025 IEEE | DOI: 10.1109/ONCON68412.2025.11384185

***Abstract*—The Finite Element Method (FEM) is a useful numerical tool for evaluating the electrical machine performance in two and three dimensions (2D and 3D), such as for the Axial Flux Machine (AFM), where the magnetic flux paths are distributed in 3D. However, as is well known, FEM is sensitive to the chosen space and time resolution (choice of mesh density and time step), and the sensitivity is highly dependent on the calculated parameters. This paper aims to quantify the considerations needed specifically when calculating the loss in Permanent Magnet (PM)s, the loss in the stator core, and the characteristics of the torque. The results show the threshold levels of mesh density and time resolution beyond which further refinement has an insignificant impact. Furthermore, this study demonstrates the selection of mesh density and time step resolution in electromagnetic transient simulations during the early stage modelling of AFMs. To validate these selections, a detailed analysis of losses and torque was conducted for a 2D, extruded 2D, and a 3D model. It was found that at no-load, the (cogging) torque in the 3D model is very sensitive to the mesh density, while at rated conditions, all models show less than 5% deviation of the average torque compared to the results with mesh and time discretization of a chosen trade-off point. Average core loss sensitivity to mesh is less than 1% when improving the mesh from medium to fine, for the 2D and 3D models, and sensitivity to time-steps is below 7% in 3D and 1% in the 2D AFM models. Magnet losses are sensitive to varying mesh density and time steps with a difference of 10% in 2D models and up to 3% for 3D models.**

***Index Terms*—Finite Element Method, Axial Flux Machines, Double Stator Single Rotor Axial Flux Machine**

I. Introduction

THE Electric Vehicle (EV) technology is rapidly transforming the transportation industry, offering sustainable and energy-efficient alternatives to traditional combustion engine vehicles. Advanced electric machine topologies like the Axial Flux Machine (AFM) are gaining attention due to a possibly lower weight and higher power density ratio. Accurate modelling of AFMs is needed for optimizing their design and the performance, and the Finite Element Method (FEM) is widely used for this purpose. Unlike the Radial Flux Machine (RFM), the flux in the AFM distributes both in the circumferential and axial direction. Hence, a 3D model of an AFM is most commonly used. The FEM simulations allow a detailed analysis of electromagnetic characteristics such as flux distribution, induced voltage, torque, and losses. However, the accuracy of the FEM models depends on space and time discretisation (mesh density and number of time-steps per electrical period). A finer mesh improves resolution, but at the expense of increased computational time and load. A balance between mesh refinement and time-step size is critical for obtaining reliable results while maintaining computational efficiency, as shown in [1] and [2] for RFMs. In [3], the significance of selecting a dense mesh and a high number of time-steps is emphasised as especially important for core and magnet loss calculations, for radial and transverse flux machines. In [4] and [5], it is highlighted that 3D AFM models provide the most accurate representation of the machine's electromagnetic behaviour, accounting for complex geometries and 3D flux paths, with higher computational costs. However, even though 2D models do not capture end effects and 3D flux variations, they offer computationally efficient alternatives with meaningful insights, especially for preliminary design, condition monitoring, and optimisation studies.

In [2], two approaches, namely, the sequential approach and iterative approach for convergence analysis, were tested with varying mesh densities on a Permanent Magnet Synchronous Machine (PMSM). The mesh density and time-steps are discretised one at a time in a sequential approach at fixed order, whereas in the iterative approach, both mesh density and time-steps are refined in cycles, by evaluating their combined impact repeatedly until the convergence criterion is met. Adaptive mesh refinement is used for local mesh refinement in [6] and [7]. In ANSYS Maxwell, transient solvers do not support adaptive meshing [8], which means that the mesh cannot be dynamically refined or remeshed during the simulation. As noted in [9], mesh quality metrics such as maximum aspect ratio, minimum orthogonal quality, and maximum skewness are more relevant for thermal modelling than electromagnetic modelling.

In [10], the torque is evaluated for different types of possible

The authors gratefully acknowledge the financial support provided by the Swedish Electromobility Center.

Authorized licensed use limited to: Chalmers University of Technology Sweden. Downloaded on February 26,2026 at 09:50:41 UTC from IEEE Xplore. Restrictions apply.

mesh combinations in the air gap of a RFM, using Coulomb's method of virtual work. In [11], a torque calculating method forAFMs was introduced and validated, showing a decreased numerical noise of the Maxwell Stress Tensor Method (MST) method when using approximate flux density fields, and lower mesh dependency with reduced computation time and memory usage.

This paper investigates the effects of mesh density and time-resolution variations on electromagnetic characteristics in AFMs. The main contribution of the paper is the quantification of the effects caused by choosing mesh density and time step resolution on key electromagnetic outputs in both 2D and 3D AFM FEM models, while outlining the methodology used to balance accuracy and computational efficiency. Previous research has explored mesh refinement and time-step resolution effects in RFMs. Quantitative evaluation of mesh and time-step induced errors in AFMs are largely unexplored, and no framework currently guides the trade-off between computational cost and simulation accuracy.

More specifically, the contribution is to exemplify the trade-offs between computational efficiency and simulation accuracy across multiple time and space discretisation levels, for Permanent Magnet (PM) loss distribution, core loss and torque characteristics such as average torque and torque ripple.

II. FEM Modelling of the AFM

The 3D FEM model of the AFM captures the complete geometry of the machine. In contrast, the 2D model simplifies the geometry, presenting it primarily as a planar structure and failing to account for three-dimensional edge effects.

A. Model Description

The Axial Flux Permanent Magnet (AFPM) machine studied is a $4kW$ Double Stator Single Rotor design with 16 poles, 18 slots, and inset PMs with an outer diameter of $166mm$. The voltage rating is $100V$, with a rated speed of $2000rpm$, and a rated torque of $19Nm$. A full 3D model and two 2D variants — a planar cross-section and an extruded model — were developed for early-stage analysis. All models shared identical geometry and were meshed with appropriate element types: tetrahedral in 3D/extruded 2D and triangular in 2D. Refinement levels were applied in regions like the air gap, teeth, and magnets. Transient simulations with varying time step resolutions (defined per electrical cycle) were performed in ANSYS Maxwell. The machine was operated at $2000rpm$ for both no load and rated case ($25A$) as in [5], to ensure a fair comparison. Some experiments were performed on the machine as described in [5] which enabled a prediction of average torque. The cogging torque was not measured but it is expected to have an average of zero. Neither the iron or magnet loss was measured. The stator material used is SURA-M235-35A [12], the rotor core material is SUS340, and the PM material is NdFeB-33UH [5] with bulk conductivity of 750469 S/m and remanent flux density of 1.2 T and coercivity of 902285 A/m.

In the 3D FEM solver in ANSYS Maxwell [8], torque is computed with the MST, where the torque acting on a rotor is obtained by taking the moment of the stress distribution over a closed surface S enclosing the rotor, see [13], with the torque τ, given by

$$\tau = \oint_S r \times (\mathbf{T} \cdot \mathbf{n}) dS \tag{1}$$

$$T_{ij} = \frac{1}{\mu_0}(B_i B_j - \frac{1}{2} B^2 \delta_{ij}) \tag{2}$$

where $\mathbf{T}$ is whole tensor matrix, T_{ij} is one of the elements of the tensor matrix $\mathbf{T}$, r is the radius of the surface S in the air gap, $\mathbf{n}$ is the normal vector of S, $\mathbf{B}$ is the magnetic flux density, and δ_{ij} kronecker delta. Further, in the 2D FEM solver in ANSYS Maxwell [8], the virtual work principle [14] is used to calculate the torque

$$\tau = \frac{\partial W'}{\partial \theta} \tag{3}$$

where dW' is the co-energy change when the rotor is moved the angle $d\theta$. Equations (1) and (3) are computed by discretizing the geometry into mesh elements, so the continuous integrals become discrete sums over these elements. Each element contributes to a torque term based on the magnetic field evaluated at its integration points. Therefore, increasing the mesh density increases the number of element contributions and hence improves the accuracy of the torque calculation.

1) 3D AFM Model

The built 3D FEM model is shown in Fig. 1 representing the full-size model and Fig. 2 representing one-quarter of the full-size model and the necessary boundary conditions. The 3D model represents the complete geometric and magnetic structure of the AFM as shown in Fig. 1. The 3D model is computationally intensive, requiring significantly higher mesh densities and finer time-steps to achieve convergence in torque, flux linkage, and induced voltage calculations. This model serves as the reference baseline in this study.

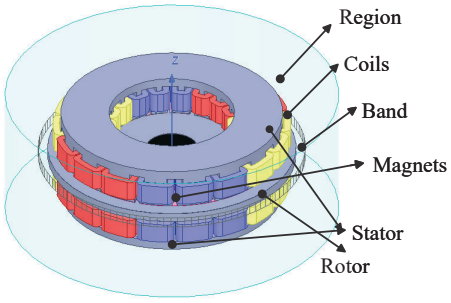

Fig. 1. 3D Model

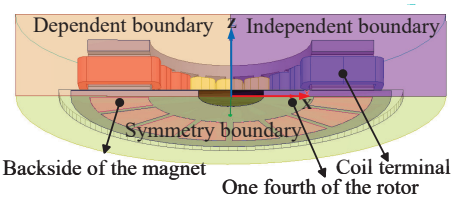

Fig. 2. Symmetrical piece of the full model with assigned boundary condition. Purple rectangle - independent boundary; Orange rectangle - dependent boundary; yellow semi-circle - symmetry boundary.

Authorized licensed use limited to: Chalmers University of Technology Sweden. Downloaded on February 26,2026 at 09:50:41 UTC from IEEE Xplore. Restrictions apply.

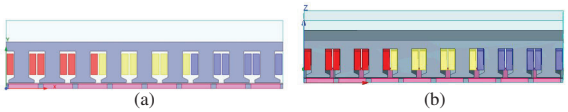

(a) (b)

Fig. 3. 2D model variants. (a) 2D model; (b) Extruded 2D model

2) 2D AFM Model

The conventional model (in the x-y-plane) was created by slicing the AFM along a radial-axial plane. This results in a simplified geometry, where only a cross-section of the machine is modelled using a planar assumption widely used as Linear Machine Modelling Approach (LMMA) as in [4] and [15]. The 2D model, as shown in Fig. 3a, reduces computational complexity and simulation time; it inherently omits radial flux distribution (along the z-axis of the 2D model), 3D fringing, and skew effects.

3) Extruded 2D AFM Model

The extruded 2D model as shown in Fig, 3b bridges the gap between the full 3D and simplified 2D models. It is constructed by extruding a 2D planar cross-section along the computational plane (the z-axis of the 2D model), forming a box, representing an angular section of the 3D model. The extruded 2D model partially captures the machine's limited radial effects, while yielding lower computational requirements than the 3D model.

III. Mesh Density and Time Step Variation in FEM Solutions

The accuracy in the solutions obtained from FEM modelling is essential, and this accuracy is influenced by varying the mesh density and time-step resolution. In this study, a hybrid mesh refinement approach is utilized, and a synchronous time-stepping method is adopted.

A. Mesh Refinement Strategy

A hybrid mesh refinement strategy is used to balance computational time with solution accuracy. The method combines Ansys Maxwell's automatic mesh scaling with manual adjustments in critical areas, such as the air gap and PM surfaces. The initial mesh, automatically created in Maxwell, is refined by fine-tuning the element sizes using both the length-based inside and outside selection options within the software. Using scaling factors with mesh element size create uniform mesh refinement across the entire geometry in both 3D and 2D models. The 3D model has a tetrahedron mesh element shape, and 2D models have triangular mesh elements. In a transient simulation, any poor-quality mesh elements present at the start will remain throughout the time-stepping process. Thus, to ensure solution accuracy with a high-quality mesh, mesh operations (such as length-based and maximum number of mesh elements) must be applied during preprocessing.

According to [8], 3D transient simulations with poor quality elements, such as with a high skew or extreme aspect ratio, can lead to significant errors in the electromagnetic field calculation whereas 2D transient models are more tolerant (but low-quality elements can still cause local inaccuracies and affect overall solution reliability). Consequently, it is essential to design the mesh carefully during pre-processing, and for this purpose scaling factors with predefined levels—extra coarse, coarse, medium, fine, and extra fine is used to allow for a consistent and quick adjustment of the mesh density.

TABLE I
MAXIMUM LENGTH OF MEDIUM MESH ELEMENT SIZE

Machine Part	Length-Based Type	Medium Mesh Element size in (mm)	
		3D (Tetra-hedral)	2D (Tri-angular)
Coils	Inside	8	5
Band	Inside	30	5
Band surface	Outside	3	2
Magnet layer	Inside	1	2
Magnet surface	Outside	2	1
Magnets	Inside	5	5
Region	Inside	40	40
Rotor	Inside	20	5
Rotor layer	Inside	10	2
Stator	Inside	15	10

TABLE II
DETAILS ABOUT THE NUMBER OF MESH ELEMENTS AND COMPUTATION TIME IN 3D AND 2D MODELS

Mesh Type/ Scaling level	3D Model		2D Model	
	Mesh elements[a]	Time[b] (hh:mm:ss)	Mesh elements[a]	Time[b] (hh:mm:ss)
Extra coarse	105865	02:01:10	3208	00:03:13
Coarse	140640	02:42:08	3872	00:03:41
Medium	353470	09:27:48	5160	00:04:37
Fine	570434	11:41:26	5997	00:05:02
Extra fine	747191	13:00:37	8573	00:06:35

[a] Total number of mesh elements
[b] Computational time to solve with total number of mesh elements

The maximum element size for each machine part is obtained by multiplying a predefined "medium" mesh element size by its scaling factor. The maximum element lengths in the machine parts with localized manual adjustments are presented in Table I. Furthermore, the defined scaling factor, the total number of mesh elements accommodated within the machine model, and the time required to solve these total mesh elements for the 3D and 2D models are listed in Table II. A visual representation of the varying mesh density in the 3D model is shown in Fig. 4.

B. Time Step Variation

The synchronous time-stepping method is adapted to capture the electromagnetic quantities where the length that the rotor moves during a simulation time step (where the time-

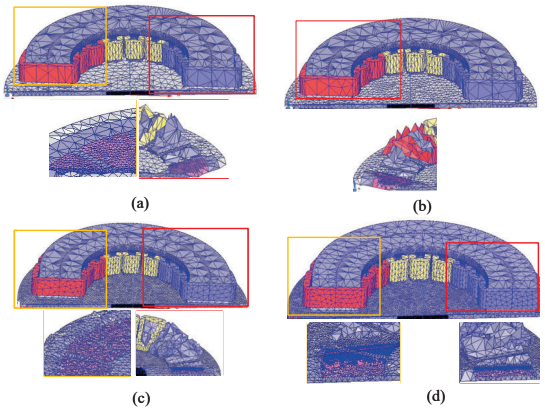

(a) (b) (c) (d)

Fig. 4. Visual representation of mesh scaling in the 3D model. (a) Extra coarse mesh - scaling factor = 3; (b) Coarse mesh - scaling factor = 2; (c) Medium Mesh - scaling factor = 1; (d) Fine mesh - scaling factor = 0.5

Authorized licensed use limited to: Chalmers University of Technology Sweden. Downloaded on February 26,2026 at 09:50:41 UTC from IEEE Xplore. Restrictions apply.

step is a percentage of the machine's fundamental electrical frequency) is synchronized with the segmentation angle of the moving band (where the band is an object that encloses all the moving parts such as the rotor core and permanent magnets and half of the air gap). Thus, in this approach, the length of the time-steps is selected to align with specific points on a sinusoidal waveform such as 0^0, 90^0, 180^0, 270^0, and 360^0 based on the desired refinement. With the mentioned angles, the number of steps per period is 4, and the number of segments on the band should consequently also be 4, so that the mesh stays the same for each time-step. This method ensures that all the electromagnetic quantities are captured at consistent and repeatable electrical angles. It is useful in electrical machines like PMSM, which are periodic systems, where excitation and response are tied to a rotating field. By aligning time-steps with the waveform cycle and with the band segmentation, errors in waveform reconstruction and output waveforms can be minimized. This leads to improved accuracy in post-processing quantities. Thus, in this study, synchronous time-stepping was implemented, and the band segmentation was adapted according to the choice of time-step. The time-steps are chosen to be 60, 120, 180, 240, or 300 steps per electric period.

C. Selection of Discretization Parameters for Loss Evaluation

Core loss at no load and magnet losses at rated conditions are evaluated with combinations of mesh density levels and time-step resolution, forming a structured 5×5 matrix of results. To discretize the parameters (mesh density levels and time-step resolution) in a systematic approach, each entry in the matrix shown in Fig. 5 corresponds to a FEM model where the losses are computed under the specified combination of mesh refinement and time-step resolution.

The average core loss (at no load) and magnet losses (at rated operation) for the described discretization points in Fig. 5 are plotted for the second period for the 2D AFM model rotated at $2000rpm$. The surface plot representation, as shown in Fig. 6, was generated to visualize the trends in

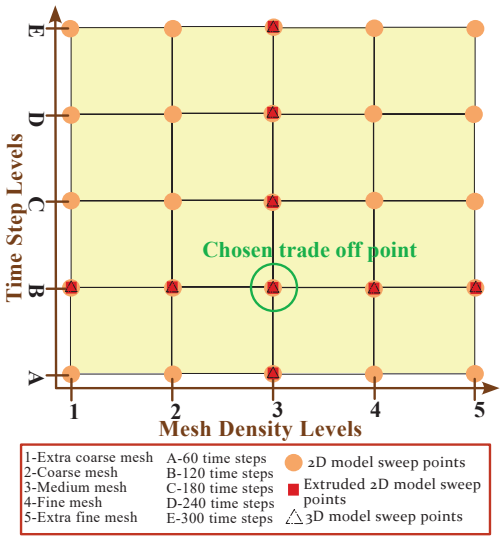

Fig. 5. Mesh density and time steps sweeping points

core loss and magnet loss variation across the discretization combinations. From the plots, it can be seen that there are differences in average losses with varying mesh density and time-steps. These plots provide insights by highlighting the regions with differences in loss values as the discretization points move towards a higher accuracy along the surface with finer mesh and higher time-step resolution, which results in higher computational time. It is seen that core loss increases with a denser mesh, whereas magnet loss decreases, and both loss components do not change much when varying the number of time-steps per period. The key here is to select a trade-off between solution accuracy and simulation time.

Based on Fig. 5 and Fig. 6, a trade-off study was conducted in the 2D model by varying mesh density and time steps, generating a 5×5 matrix of simulations. A medium mesh with 120 time steps was selected as the optimal point, balancing accuracy and computational time, and this choice was verified with the 3D and extruded 2D model for torque and loss simulations. In Fig. 6, it can for example be seen that a decrease in number of time-steps compared to the trade-off point, will not change the result of the core loss much, whereas it will change the the results of the magnet loss notably. If instead increasing the number of time-steps (and the simulation time), both the magnet and core loss does not change much. Having the choice of time-step of the trade-off point (120 steps per period) also shows that the change in mesh does not influence the solution time much, and the trade-off point regarding the mesh can be chosen more freely, at least for the 2D model.

IV. Results and Discussions

At no-load, minimal magnetic field variation allows accurate results with coarser meshes, though edge details may be lost. Under rated conditions, high currents induce complex, non-linear fields, requiring finer meshes, especially in critical regions like the air gap.

A. Impact on Torque

At no-load, the average torque of the 3D and 2D models varies notably with mesh density, as seen in Fig. 7. Ideally, the average cogging torque should be zero, but a dense mesh fails to capture this. Even with a higher mesh density, the torque differs in the 2D and 3D simulations, since the 2D model neglects the tapered (trapezoidal) shape of the stator teeth and magnets.

In Fig. 8, the average torque for rated conditions is presented for all three models when varying the mesh density with 120 time-steps (see Fig. 8a) and the time resolution with medium mesh density (see Fig. 8b). In rated condition, the 2D model shows barely any difference in the accuracy of the measured average torque with varying time-steps. Similarly, when varying the time-steps, the 3D model shows negligible differences. Regarding the mesh, the percentage difference in average torque between the medium mesh compared to the extra coarse mesh is about 3% ($20.33Nm$ versus $21.04Nm$), while the difference compared to the extra fine mesh (yielding $20.38Nm$) is less than 0.3%. For the 2D model, the percent-

Authorized licensed use limited to: Chalmers University of Technology Sweden. Downloaded on February 26,2026 at 09:50:41 UTC from IEEE Xplore. Restrictions apply.

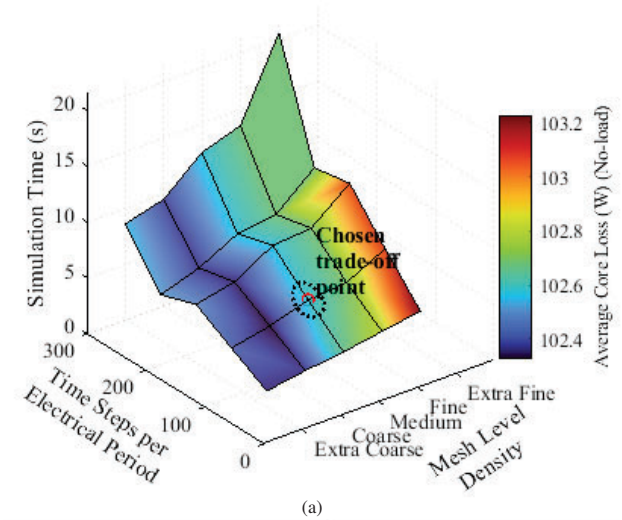

(a)

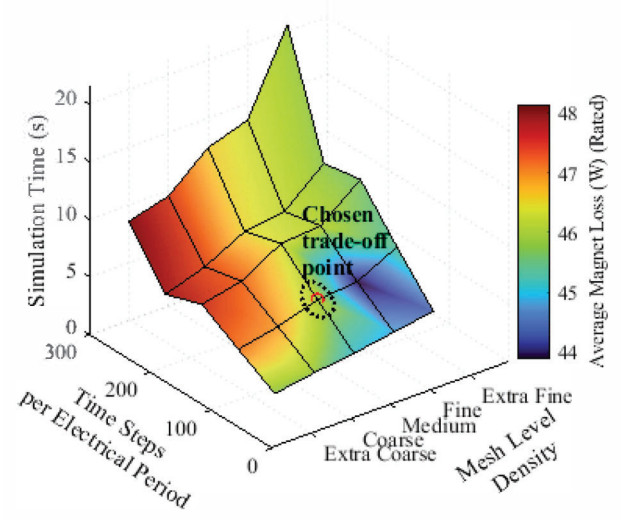

(b)

Fig. 6. Average core loss at no-load and average magnet loss at rated operation with varying mesh density and time steps. (a) Average core loss in 2D model at no-load; (b) Average magnet loss in 2D model at rated operating point

age difference between the trade-off point (medium mesh), extra coarse mesh, and extra fine mesh remains below 1% (20.28Nm, 20.31Nm, and 20.25Nm). Hence, the accuracy of the measured average torque is quite stable in the rated case.

B. Impact on Core Loss

Fig. 9 presents the average core loss at no-load and rated conditions across all three models under varying mesh densities with 120 time steps and varied time resolutions with medium mesh density. As seen in Fig. 9a, medium to fine meshes result in a difference of less than 1% for both the 2D and 3D models (for the no load case: 101W versus 102W for 3D; 102W versus 103W for 2D), while extra coarse meshes lead to about 20% deviation (132W versus 106W for the rated case and 130W versus 101W for the no load case in the 3D model) due to poor flux density resolution, but the deviation reduces as the mesh is refined. In Fig. 9b, the average core loss at rated conditions at different time-steps deviates by just 0.8% in 2D (104.9W versus 104.1W), whereas 3D shows

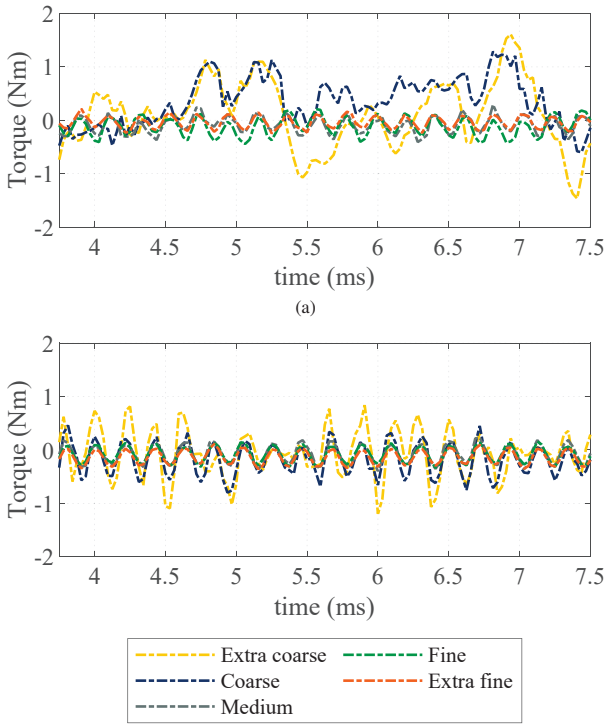

(a)

(b)

Fig. 7. Torque vs Time at no load (cogging torque) with variation in mesh density. (a) 3D Model; (b) 2D Model

2%–7% relative to the trade-off point for the rated operating point with 120 time-steps (103W for 60 time-steps and 108W for 300 time-steps), highlighting higher sensitivity to time resolution in the 3D models. At no-load, core loss remains nearly unchanged in 2D, while 3D shows minor variations less than 2%. Hence, time-steps of 120 are quite a reasonable choice from the accuracy and computational time perspective.

C. Impact on Permanent Magnet Loss

Magnet losses arise from the interaction between time-varying magnetic fields and the conductive materials within the magnet. These losses are influenced by spatial variations in the magnetic flux density, dynamic field changes (in rated conditions), and localized hotspots. These localized hotspots can be due to eddy current concentration, especially in areas of high flux density gradients, such as the magnet edges.

Fig. 10 illustrates the differences in representation of magnet eddy currents among the three models. The 3D model uses trapezoidal PMs, producing complex flux gradients and varying eddy current paths. In contrast, the extruded 2D model uses rectangular magnets with the same cross-sectional area, while the 2D model simplifies the PM to a line. Though 2D and 3D models show similar loss trends due to circulating eddy currents within the magnets, the 2D model oversimplifies the current paths and neglects 3D effects like leakage flux and edge gradients. As a result, loss prediction accuracy drops, with deviations above 35% in rated conditions compared to the 3D model (for example about 46W in 2D and 30W in 3D at a medium mesh and 120 time-steps).

Authorized licensed use limited to: Chalmers University of Technology Sweden. Downloaded on February 26,2026 at 09:50:41 UTC from IEEE Xplore. Restrictions apply.

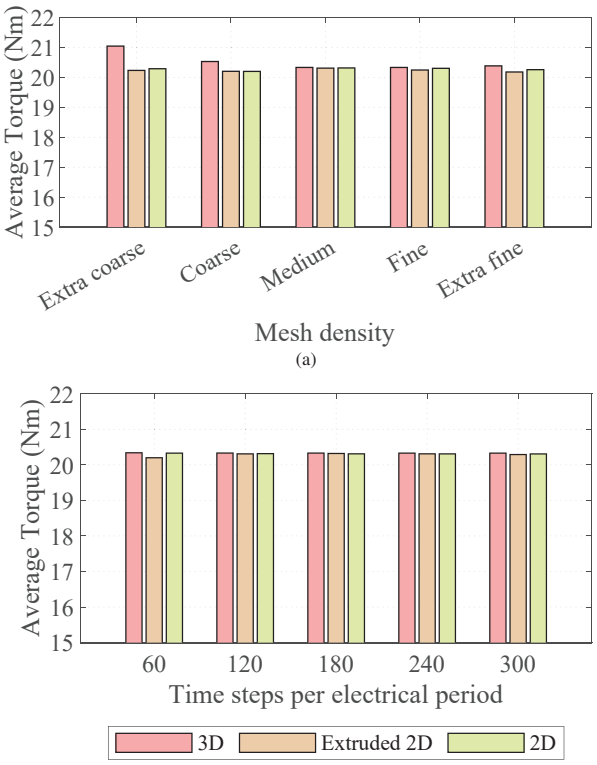

Fig. 8. Average torque at rated operation with varying mesh density and time steps (zoomed in view between 15-22Nm). (a) Average torque rated operation with varying mesh density; (b) Average torque at rated operation with varying time steps

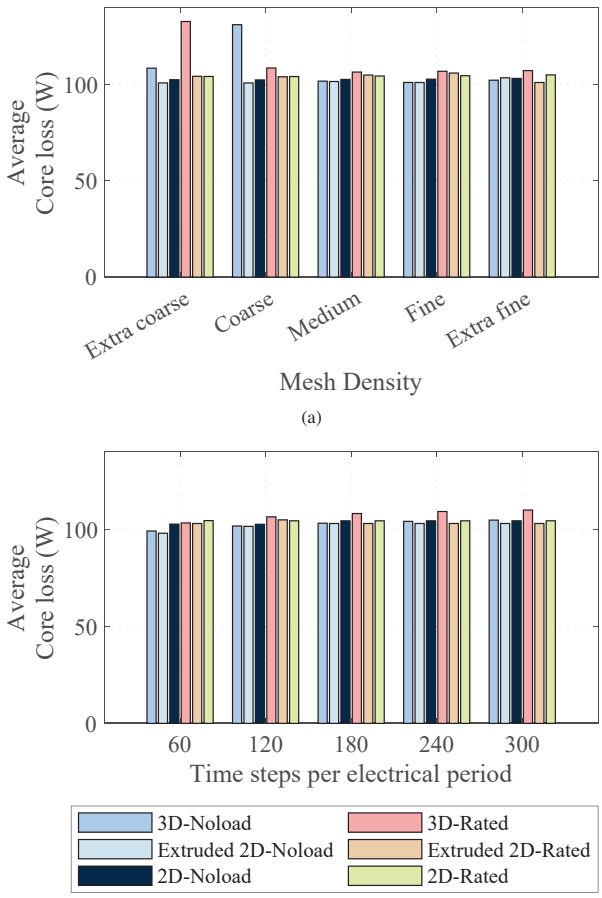

Fig. 9. Core loss in 3D, extruded 2D, and 2D models with variation in mesh density and time steps. (a) Average core loss with varying mesh density; (b) Average core loss with varying time steps

Thus, in 3D models, magnetic field variations in all directions (radial, tangential, axial) are captured, enabling accurate computation of eddy-current-based magnet losses, especially under rated conditions with complex, localized fields. In contrast, 2D models simplify geometry and assume symmetry, neglecting effects like fringing, leakage, and edge gradients. This leads to reduced accuracy in predicting solid losses.

From the mesh density variation investigation, it is seen in Fig. 11a that the magnet losses are quite sensitive to the choice of mesh in both the 3D and 2D models. A similar trend can be observed in Fig. 11b regarding the variation of time-steps. The differences in accuracy of the average magnet losses for the 3D and 2D models range between 3% to 10% for the rated case, where the 2D shows a higher sensitivity to both mesh and time step variation compared to the 3D model. Owing to the differences in accuracy, the selected trade-off point is considered reasonable.

V. Conclusion

This study systematically examined the sensitivity of electromagnetic loss calculations to mesh density and time-step settings across 2D, extruded 2D, and 3D models. Surface plots were utilized to map losses across a structured 5×5 matrix of mesh density and time step combinations, facilitating identification of a suitable trade-off point. This visualization helped highlight the areas with a good balance between accuracy and computation time. The selected trade-off point was validated for core loss, PM loss, and torque. The torque deviations at rated conditions were below 5% for both 3D and 2D models, while only the 3D model exhibited instability at no-load under a coarser mesh. Core losses remained consistent with deviations under 1% in both models while varying the mesh density and the sensitivity to time-steps is below 7% in 3D models and 1% in 2D AFM models. For magnet losses, 3D and 2D models showed sensitivity to mesh density and time step variation of 10% in 2D models and up to 3% for 3D models. The differences in the magnet losses between the

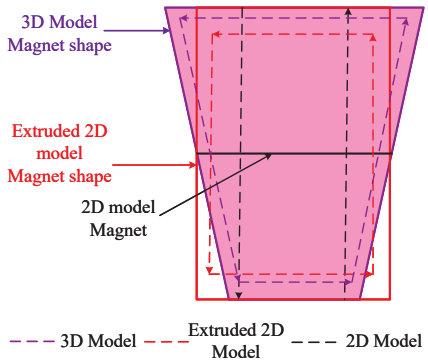

Fig. 10. Eddy currents in magnets for different models

Authorized licensed use limited to: Chalmers University of Technology Sweden. Downloaded on February 26,2026 at 09:50:41 UTC from IEEE Xplore. Restrictions apply.

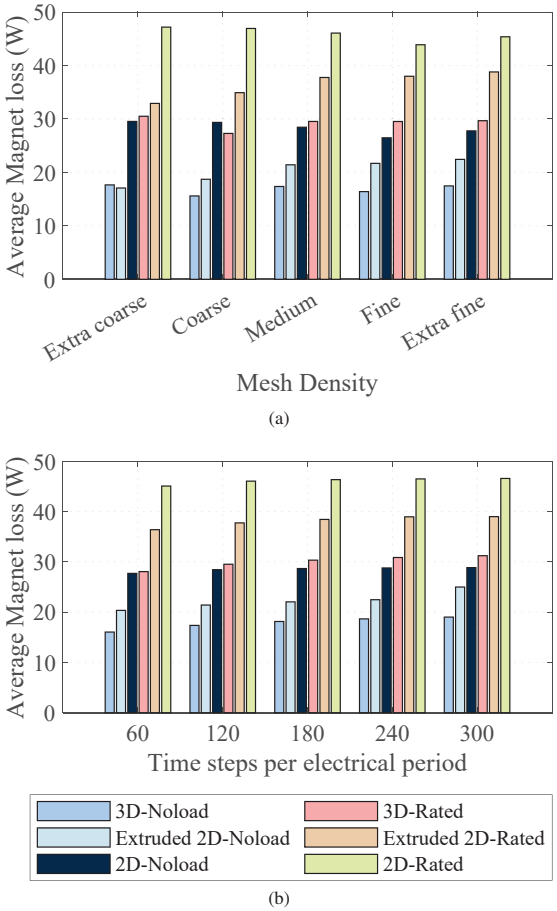

Fig. 11. Magnet loss in 3D, extruded 2D, and 2D models with variation in mesh density and time steps. (a) Average magnet loss with varying mesh density; (b) Average magnet loss with varying time steps

3D and the 2D model are explained. In the entire study, the accuracy of the losses and torque largely depended on the selection of mesh density compared to the selection of time-steps. The results from the extruded 2D model highlighted the difference in the results due to different solvers in 3D and 2D FEM modelling. This methodology offers a practical and visually guided framework for selecting discretization parameters in early-stage FEM design of AFMs. Future work will focus on extending the current study to mesh and time step investigation on design modifications, and perform more experimental verification of the FEM results to further validate the numerical predictions.

REFERENCES

[1] Elisabet Jansson, Torbjörn Thiringer, and Emma Grunditz. "Time Resolution Dependency of Core Loss Accuracy in Finite Element Analysis of a Permanent Magnet Synchronous Machine". In: *2020 International Conference on Electrical Machines (ICEM)*. Vol. 1. IEEE. 2020, pp. 1011–1017.

[2] Elisabet Jansson, Torbjörn Thiringer, and Emma Grunditz. "Convergence of core losses in a permanent magnet machine, as function of mesh density distribution, a case-study using finite-element analysis". In: *IEEE Transactions on Energy Conversion* 35.3 (2020), pp. 1667–1675.

[3] Sonja Tidblad Lundmark and Poopak Roshanfekr Fard. "Two-dimensional and three-dimensional core and magnet loss modeling in a radial flux and a transverse flux PM traction motor". In: *IEEE Transactions on Industry Applications* 53.3 (2017), pp. 2028–2039.

[4] Vineetha Puttaraj, Sonja Tidblad Lundmark, and Torbjörn Thiringer. "Moving from a 3D Axial Flux Machine Model to 2D Considering the Impact of End Leakage Flux". In: *2024 International Conference on Electrical Machines (ICEM)*. IEEE. 2024, pp. 1–7.

[5] Vineetha Puttaraj. "Modeling of a 4kW Axial Flux Machine-Measurements and 2D/3D Modeling". Licentiate thesis. Sweden: Chalmers University of Technology, 2025.

[6] Alexey Belokrys-Fedotov et al. "Adaptive Mesh Refinement for Electromagnetic Simulation". In: *International NUMGRID Conference*. Springer. 2022, pp. 123–147.

[7] Katsumi Yamazaki and Toshihiro Saeki. "Adaptive mesh generation within nonlinear iterative calculations for analyses of electric machines". In: *IEEE transactions on magnetics* 39.3 (2003), pp. 1654–1657.

[8] Ansys Inc. *ANSYS Maxwell 3D User Manual*. Version 25.1. [Online; accessed 12-Sep-2025]. 2024. URL: https://ansyshelp.ansys.com/public/account/secured?returnurl=/Views/Secured/Electronics/v252/en/Subsystems/Maxwell/Maxwell.htm.

[9] Sonja Tidblad Lundmark et al. "Heat transfer coefficients in a coupled 3-D model of a liquid-cooled IPM traction motor compared with measurements". In: *IEEE Transactions on Industry Applications* 57.5 (2021), pp. 4805–4814.

[10] Bishal Silwal et al. "Computation of torque of an electrical machine with different types of finite element mesh in the air gap". In: *IEEE Transactions on Magnetics* 50.12 (2014), pp. 1–9.

[11] Josefina María Silveyra and Juan Manuel Conde Garrido. "Torque calculation method for axial-flux electrical machines in finite element analysis". In: *Finite Elements in Analysis and Design* 227 (2023), p. 104042.

[12] SURA-M235-35A. *Material data for SURA M235-35A steel*. Accessed:Dec 2024. URL: https://e-magnetica.pl/database-em/01_Soft/Electrical_steels/Cogent_Newport_2003/NO-11.pdf.

[13] John David Jackson. *Classical Electrodynamics*. 3rd. Chapter 6: Stress Tensor. New York, USA: Wiley, 1998.

[14] J-L Coulomb and G Meunier. "Finite element implementation of virtual work principle for magnetic or electric force and torque computation". In: *IEEE Transactions on magnetics* 20.5 (2003), pp. 1894–1896.

[15] Mehmet Gulec and Metin Aydin. "Implementation of different 2D finite element modelling approaches in axial flux permanent magnet disc machines". In: *IET Electric Power Applications* 12.2 (2018), pp. 195–202.

Authorized licensed use limited to: Chalmers University of Technology Sweden. Downloaded on February 26,2026 at 09:50:41 UTC from IEEE Xplore. Restrictions apply.